Наносистеми, наноматеріали, нанотехнології
Nanosistemi, Nanomateriali, Nanotehnologii
2026, т. 24, № 2, сс. 455–467
https://doi.org/10.15407/nnn.24.02.0455

PACS numbers: 73.20.Mf, 78.20.Ci, 78.40.-q, 78.67.Bf, 79.20.Eb, 81.15.Fg, 81.16.Mk

Irradiation Effect on the Optical Properties of Silver Nanoparticles Prepared by Pulsed-Laser Ablation in Liquid

Moumen Al-Azow, Mushtaq Abed Al-Jubbori, and Ivan B. Karomi

College of Education for Pure Sciences,
Department of Physics,
University of Mosul,
41001 Mosul, Iraq

In this work, colloidal silver nanoparticles (Ag NPs) are prepared using the pulsed-laser ablation in liquid (PLAL) technique. The study is focused on clarifying the effect of the number of laser pulses used on the optical properties of nanoparticles of high-purity silver targets immersed into 5 mL of deionized distilled water. The laser used is a Nd:YAG *Q*-switched laser with a fixed energy of 260 mJ, a wavelength of 532 nm, a pulse duration of 10 ns, and a frequency of 1 Hz. 100, 200, and 300 pulses are used to prepare the nanoparticles. The prepared particles are then irradiated with energy of 260 mJ and a set of 300 pulses of ultraviolet UVC rays with time intervals of 1–5-hour increments of one hour each time. The effect of UV-irradiation times on colloidal nanoparticles is studied through optical absorption and optical energy-gap analysis. The behaviour of the UV and visible absorption spectra of silver nanoparticles is also studied as functions of wavelength and number of pulses. These results show that the intensity of absorbance increases with an increase in the number of pulses, and this indicates an increase in the concentration of nanoparticles. As also noted, Ag NPs have a single sharp absorption peak between 404–407 nm for an energy of 260 mJ. Through the absorption spectrum, the optical energy gap is also calculated for Ag NPs; the calculations show an increase in the power value with increasing number of laser pulses. Optical constants are also calculated, and it is observed that their values increased with increasing number of laser pulses. On the other hand, the results of the UV–Vis absorption spectrum show a decrease in the absorption peaks as functions of the time of ultraviolet irradiation.

У цій роботі колоїдні наночастинки срібла (Ag НЧ) було одержано за допомогою методу імпульсної лазерної абляції в рідині (PLAL). Дослідження зосереджено на з'ясуванні впливу кількости використаних лазерних імпульсів на оптичні властивості наночастинок високочистих срібних мішеней, занурених у 5 мл дейонізованої дистильованої води.

Використаний лазер — це Nd:YAG-лазер з модуляцією добротности з фіксованою енергією у 260 мДж, довжиною хвилі у 532 нм, тривалістю імпульсу у 10 нс та частотою в 1 Гц. Для одержання вищезгаданих наночастинок використовувалося 100, 200 та 300 імпульсів. Потім підготовлені частинки опромінювали з енергією у 260 мДж і кількістю по 300 імпульсів ультрафіолетових UVC-променів (із довжинами хвилі у 100–280 нм або 200–280 нм) з часовими інтервалами у 1–5 годин інкрементів упродовж однієї години кожного разу. Вплив часу УФ-опромінення на колоїдні наночастинки вивчали за допомогою аналізи оптичного вбирання й оптичної забороненої енергетичної зони. Також вивчали поведінку УФ- і видимих спектрів вбирання наночастинок срібла як функції довжини хвилі та кількости імпульсів. Ці результати показали, що інтенсивність вбирання зростає зі збільшенням кількости імпульсів, і це вказує на збільшення концентрації наночастинок. Також було зазначено, що Ag НЧ мають єдиний різкий пік вбирання між 404–407 нм для енергії у 260 мДж. За допомогою спектру вбирання також було розраховано оптичну заборонену зону для Ag НЧ; розрахунки показали збільшення значення потужности зі збільшенням кількости лазерних імпульсів. Також було розраховано оптичні константи і було спостережено, що їхні значення збільшуються зі збільшенням кількости лазерних імпульсів. З іншого боку, результати стосовно спектру вбирання UV–Vis показали зменшення піків вбирання як функцій часу ультрафіолетового опромінення.

Key words: Ag nanoparticles, optical properties, laser ablation, UVC irradiation.

Ключові слова: наночастинки срібла, оптичні властивості, лазерна абляція, ультрафіолетове UVC-опромінення.

(Received 19 October, 2024; in revised form, 20 October, 2024)

1. INTRODUCTION

Materials, which are described as nanomaterials, are those that typically have at least one dimension of less than 100 nm [1]. Their size and form have a significant influence on their unique physicochemical features.

The reason for the revolution in nanomaterials' manufacturing processes and their widespread use in various scientific and technological fields is their novel features, which set them apart from the corresponding bulk material [2].

Through material manipulation at the nanoscale, materials can be made to have extremely precise surface areas as well as better mechanical, optical, magnetic, and other capabilities. This has led to the emergence of several exciting new research directions [3].

In most industrial areas, the process of assembling nanostruc-

tures using various techniques known as nanofabrication has become quite popular [4].

Nanostructures can be created using a variety of strategies and processes. The two main categories of methods for nanofabrication are 'top down' methods, which involve reducing the starting material to the desired sizes through physical or chemical methods like electron or ion beam, milling, laser ablation, and reactive ion etching, and 'bottom-up' methods, which involve assembling individual atoms or molecules to obtain the final nanostructure. Examples of this strategy include chemical and physical vapour deposition (CVD and PVD), epitaxial growth, self-assembly, *etc.* [5, 6].

Laser ablation is one of the many nanofabrication processes available. It is an environmentally benign method of synthesizing nanomaterials with several exceptional features, including high production efficiency, low cost, good stability, and consistent processing quality [7]. Numerous nanomaterials and nanostructures with enhanced chemical, optical, magnetic, and electrical capabilities have been created using this method.

Chemical vapour deposition (LCVD), pulsed laser deposition (PLD), laser ablation, laser vaporization, and other laser-based processes are being utilized to create nanoscale materials with precise dimensions, forms, and characteristics [8]. Laser synthesis and processing of colloids (LSPC) is another scalable and adaptable laser-based method for processing nanomaterials that has a significant impact on nanotechnology. This method can be divided into three categories: laser ablation in liquids (LAL), which creates colloidal nanoparticles by continuously scanning a bulk target in liquid; laser fragmentation in liquids (LFL), which uses lasers to fracture colloidal nanoparticles' or microparticles' suspensions; and laser melting in liquids (LML), which uses the laser beam to melt primary nanoparticles into larger ones [9].

In this work, a pulsed laser was used to synthesis silver nanoparticles (Ag NPs) immersed in water to study it optical and physical properties and the extent of their effect on irradiation. Ag NPs have drawn attention due to their optical, electrical, and magnetic capabilities [10–14]. Ag NPs display novel optical characteristics not found in bulk metals or molecules.

The existence of an absorption band in the visible-light spectrum is one such. The appearance of this band is caused by conduction-electron surface plasmons' oscillation modes, which are connected to external electromagnetic fields through the surface [15]. Ag NPs are perfect for molecular labelling because of their surface-plasmon resonance and wide effective scattering cross section, which allow for the observation of phenomena like surface-enhanced Raman scattering take advantage of Ref. [16].

2. EXPERIMENTAL METHODS

2.1. Synthesis Methods of Silver Nanoparticles

A high-purity silver disk of 21 mm in diameter and 2 mm thick was used. The sample was cleaned and impurities were removed by washing it with distilled water after immersing it in liquid ethanol for 10 min. The target was placed in a beaker glass containing 5 ml of distilled water (DW). The distilled water was approximately 4 mm above the target surface. The beaker was rotated by using an electric motor around. Figure 1 depicts the PLAL-process experiment setup. Nanosecond laser pulses were used to ablate an Ag target, resulting in slimy Ag NPs in deionized water. A *Q*-switched Nd:YAG laser beam (of 532 nm wavelength with pulse duration of 10 ns, and repetition rate of 1 Hz) with ablation energy constant of 260 mJ and different pulses' number (100, 200, and 300 pulses).

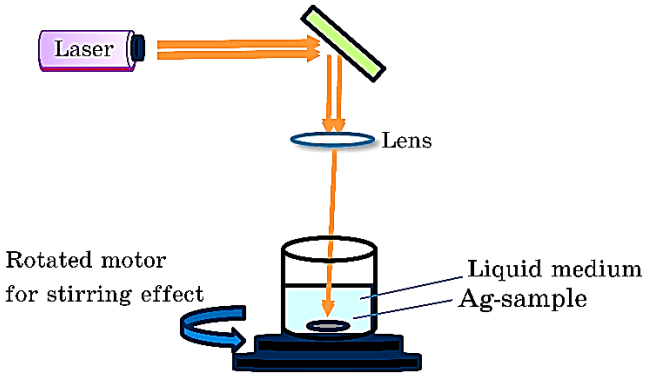

Fig. 1. Schematics of PLAL set up for the synthesis of Ag NPs in liquid.

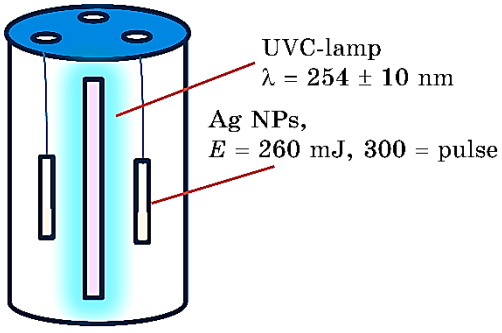

Fig. 2. UVC-irradiation diagram.

2.2. UVC Irradiation of Ag NPs

Ag NPs samples were exposed with 300 pulses of 260 mJ to a 254 ± 10 nm wavelength of ultraviolet (UVC) radiation in order to characterize the synthesized Ag nanoparticles. The UVC-irradiation system is comprised of 1 m long and 20 cm diameter tube. As depicted in Fig. 2, the tube contains a lamp in the centre and is covered tightly at its base. The samples are irradiated in a darkroom at intervals of 1–5 hour in steps of 1 hour. Optical absorption measurements were performed immediately to study the effect of UVC irradiation on Ag NPs.

3. RESULTS AND DISCUSSIONS

3.1. Ag Nanocolloid Characterization

The optical absorption spectra of colloidal Ag NPs were measured immediately after ablation using a Shimadzu UV-1800 double-beam UV–Vis spectrophotometer with a scanning range of 190–1100 nm. The quantity of absorption in colloidal solutions created with 260-mJ pulse-laser energy is dependent on the number of laser pulses. A phenomenon known as 'plasmon absorption' caused the colour of the colloidal silver nanoparticles to change to a Pale yellow.

The increase in absorption with an increasing number of laser pulses indicates an increase in Ag NPs' concentration. The surface-plasmon resonance peak increases, indicating the presence of nanoscale Ag particles, as shown in Fig. 3.

The absorption coefficient (α) was calculated from the absorbance spectrum, and we notice from the results we obtained (Fig. 4) that, when the number of pulses increases, the peak of the absorption coefficient spectra increases as a function of the wavelength in the visible region of the silver nanoparticles, as it was observed that the edge of the absorption coefficient of these particles increases from $2.28 \cdot 10^4$ cm^{-1} to $8.27 \cdot 10^4$ cm^{-1} (this is due to the increase in nanoparticles' concentration with increasing number of pulses).

The transmission (T) and reflection (R) spectra are related to the absorption coefficient (α), according to Beer's law [17, 18]:

$$\alpha = \frac{1}{d} \log \left[\frac{(1-R)^2}{2T} + \frac{(1-R)^2}{(\sqrt{2T^2 + R^2})} \right], \qquad (1)$$

where d is the thickness of the sample.

This work also studied some of the optical constants of silver nanoparticles and demonstrated the effect of the number of pulses on their values.

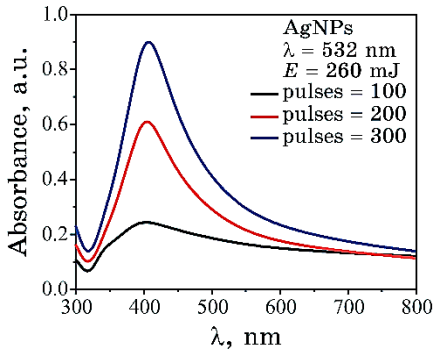

Fig. 3. The absorption spectra of Ag NPs in distilled water for 100, 200, and 300 laser pulses with energy of 260 mJ.

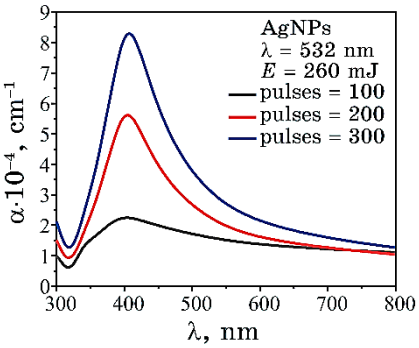

Fig. 4. Absorption coefficient of Ag NPs as a function of wavelength for 100, 200, and 300 pulses at energy of 260 mJ.

We start with the refractive index (n), which was calculated through Eq. (2) [17, 18]:

$$n = \frac{1+R}{1-R} + \sqrt{\frac{4R}{(1-R)^2} - K^2}\ . \qquad (2)$$

As observed in Fig. 5, the value of the refractive index increases with the increase in the number of pulses and reaches its highest value in the visible region of the spectrum. The amount of increase from 1.94 to 2.61 was at the lowest and highest number of pulses. This increase is due to an increase in the concentration of nanoparticles with an increase in the number of ablation pulses.

Reflectivity is calculated from absorption and transmission spectra using the law of conservation of energy ($R = 1 - T - \mathrm{A}$).

The reflection-coefficient values were also estimated as a function of wavelength; as shown in Fig. 5, *b*, its value increases from 0.103

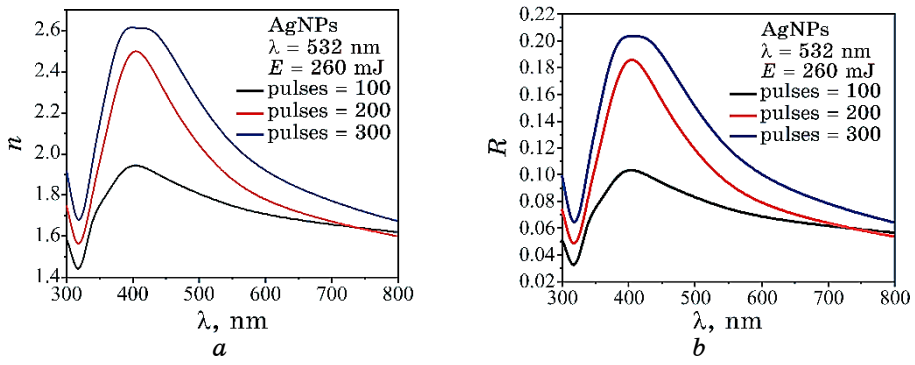

Fig. 5. (*a*) Refractive index (n) and (*b*) reflection coefficient (R) as functions of wavelength for 100, 200, and 300 pulses at energy of 260 mJ.

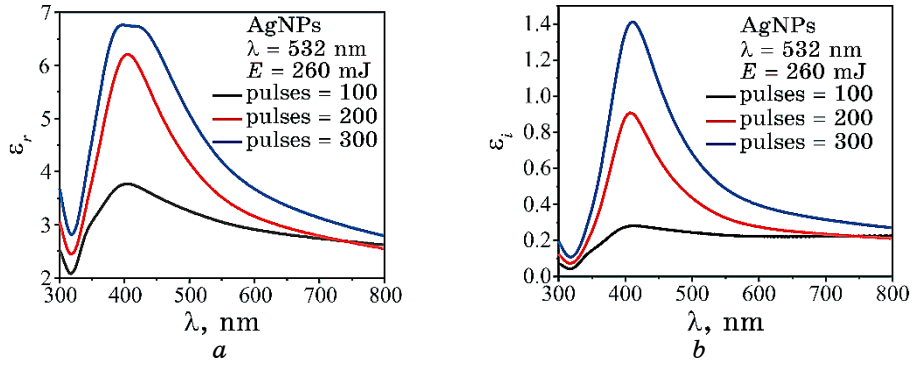

Fig. 6. (*a*) Real dielectric constant (ε_r) and (*b*) imaginary dielectric constant (ε_i) as functions of wavelength for 100, 200, and 300 pulses at energy of 260 mJ.

to 0.20 with an increase in the number of pulses. The reason for this may be due to the increase in the nanoparticles' concentration.

The real and imaginary electrical dielectric constants (ε_r) and (ε_i) were calculated using Eqs. (3) and (4), respectively [18]:

$$\varepsilon_r = n^2 - K^2, \tag{3}$$

$$\varepsilon_i = 2nK. \tag{4}$$

Figure 6, *a* and *b* show a difference in their values as functions of wavelength; as it was observed, there is an increase in their values with an increase in the number of pulses in the visible region of the spectrum (this is due to the increased concentration of nanoparticles).

Figure 7, *a* shows the change in the extinction coefficient (K) as

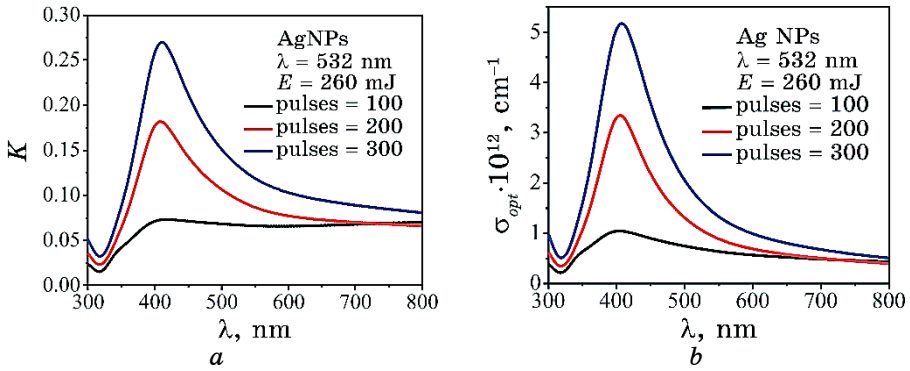

Fig. 7. (*a*) Extinction coefficient (*K*) and (*b*) optical conductivity ($\sigma_{opt.}$) as functions of wavelength for 100, 200, and 300 pulses at energy of 260 mJ.

a function of the wavelength for the silver nanoparticles, which was calculated using Eq. (5) [18]:

$$K = \frac{\alpha\lambda}{4\pi}. \tag{5}$$

An increase in the peak values of the extinction coefficient in the visible region of the spectrum was observed with an increase in the number of pulses, as the peak values of the extinction coefficient range between 0.07–0.27 (and this is due to the reason that this increase leads to an increase in the laser ablation rate with an increase in the number of pulses).

Optical conductivity values (σ) as a function of wavelength were also calculated through Eq. (6) [19]:

$$\sigma = \frac{\alpha n c}{4\pi}, \tag{6}$$

where *c* is the speed of light in a vacuum.

As shown in Fig. 7, *b*, the value of optical conductivity increases with the increase in the number of pulses. This increase may be attributed to the creation of new levels within the band gap that facilitates the crossing of electrons from the valence band to these levels and, then, to the conduction band [20].

The optical energy gap ($E_g^{opt.}$) of Ag NPs was estimated from ultraviolet-spectroscopy data with using the Tauc's Eq. (7) [21]:

$$(\alpha h\nu)^{1/i} = k\left(h\nu - E_g^{opt.}\right), \tag{7}$$

where $h\nu$ is the energy of the incident photons, *i* takes values of 1/2 or 3/2 for direct transitions, whereas for indirect transitions, it

takes 2 or 3, depending on whether they are allowed or forbidden, respectively. (k is a constant of effective mass.)

Figure 8 shows a slight increase in the value of the energy gap with an increase in the number of pulses. Figure 9 also shows the increase in energy gap with increasing number of pulses. From this,

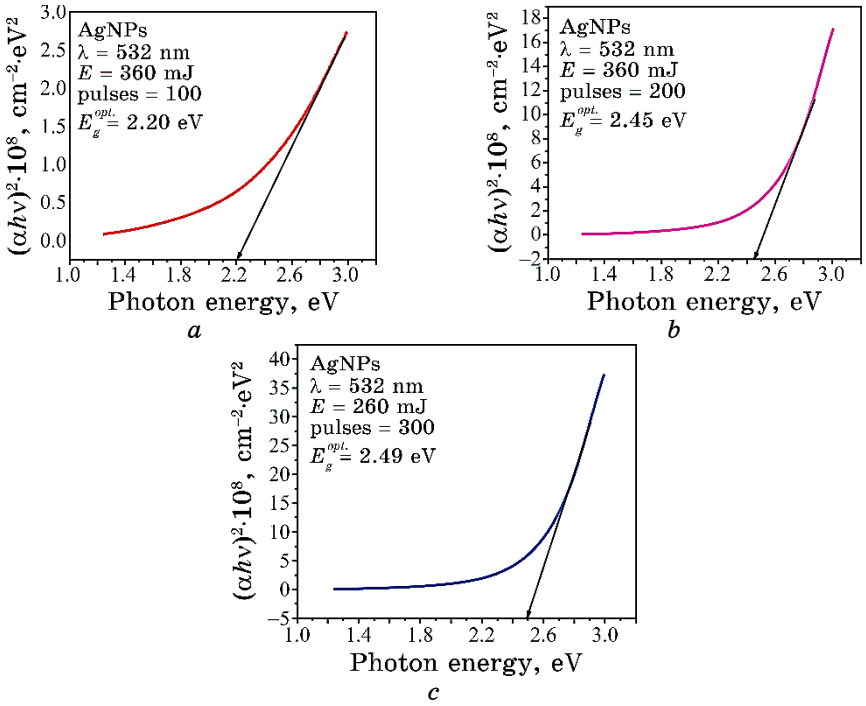

Fig. 8. Optical band gap values for Ag NPs for different numbers of pulses: (*a*) 100, (*b*) 200, (*c*) 300.

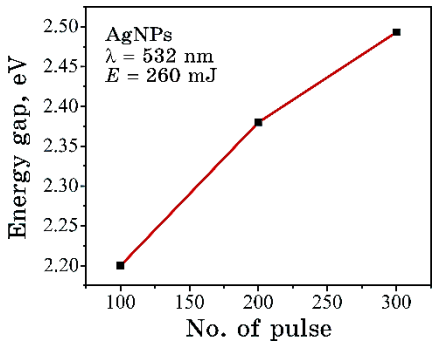

Fig. 9. Energy gap as a function of a number of pulses.

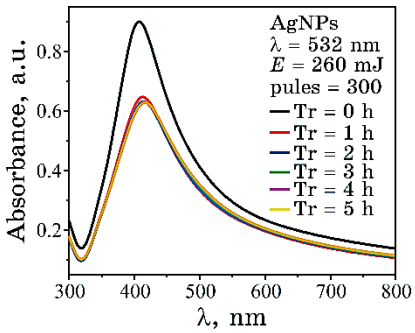

Fig. 10. Absorption spectrum as a function of wavelength after UV irradiation for Ag NPs prepared with 300 pulses at energy of 260 mJ.

we conclude that there is a decrease in the size of the extracted nanoparticles.

3.2. Effect of UVC Irradiation on the Optical Properties of Ag NPs

The samples were exposed to UVC irradiation for varying durations. We notice in Fig. 10 that the absorbance decreases with increasing irradiation time, and this may be due to the increased dispersion of nanoparticles.

It was also observed in Fig. 11 that the optical energy gap decreases slightly with increasing time irradiation. This may be due to some electrons gaining energy with increasing irradiation time, capable of being transferred from the valence band, and, thus, forming a new band above it that leads to a decrease in the energy gap.

Figure 12 also shows the decrease in energy gap with increasing irradiation time.

4. CONCLUSIONS

Through this work, the possibility of producing colloidal silver nanoparticles is investigated using the pulsed laser ablation (PLAL) technique. The results demonstrate that Ag NPs can be obtained using an Nd:YAG laser with a wavelength of 532 nm and for different numbers of pulses. The colour change of the solution and the analysis of the absorption spectrum are preliminary evidence of the formation of the nanomaterial.

The energy gap is also calculated, and it is found that it increases with an increase in the number of pulses.

The effect of irradiation on the optical properties of the fabricated nanoparticles is also studied, and it is found that, in general, the

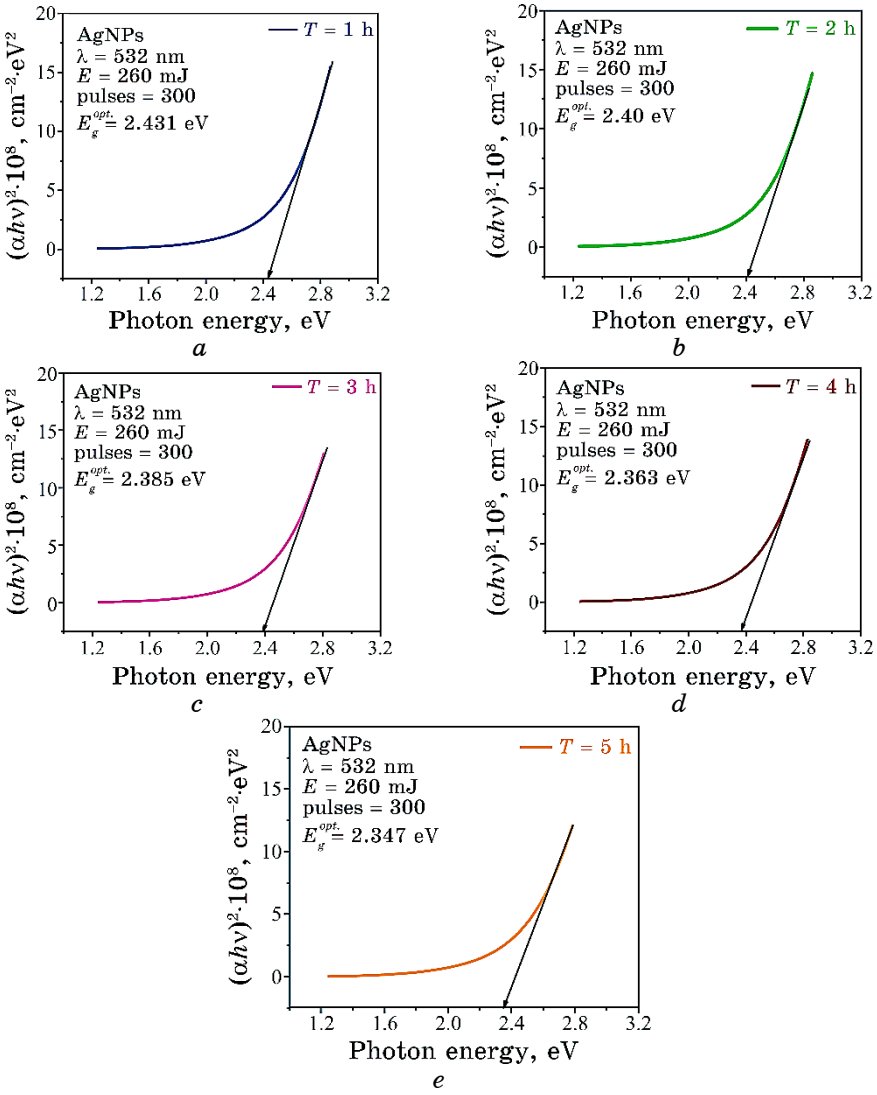

Fig. 11. Optical energy-gap spectrum of Ag NPs for different UV-irradiation times prepared with 300 pulses at energy of 260 mJ.

absorption spectrum decreases with increasing irradiation time.

ACKNOWLEDGMENTS

We thank University of Mosul, College of Education for Pure Sciences and Department of Physics for supporting this work.

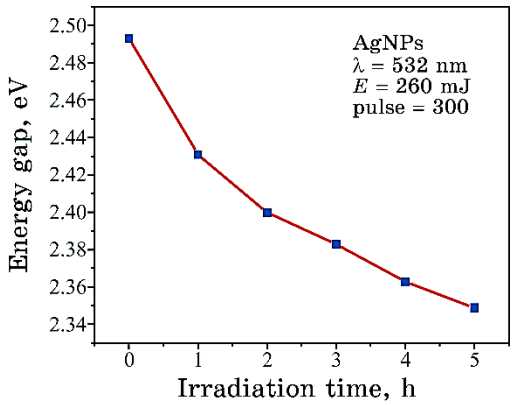

Fig. 12. The energy gap as a function of UV-irradiation time.

REFERENCES

1. Noor Atalla Al-Jubbori and Mushtaq Abed Al-Jubbori, *Journal of Education and Science*, **31**, No. 2: 1 (2022); doi:10.33899/edusj.2022.132843.1212
2. Mushtaq Abed Al-Jubbori, Omar Ayed, and Khalaf Ajaj, *Radiation Physics and Chemistry*, **226**: 112190 (2025); https://doi.org/10.1016/j.radphyschem.2024.112190
3. Noor Atallal Al-Jubbori and Mushtaq Abed Al-Jubbori, *Journal of Education and Science*, **31**, No. 2: 105 (2022); doi:10.33899/edusj.2022.133494.1229
4. Mohamed Boutinguiza Larosi, Jesús del Val García, and Antonio Riveiro Rodríguez, *Nanomaterials*, **12**, Iss. 17: 2903 (2022); https://doi.org/10.3390/nano12172903
5. Namra Abid, Aqib Muhammad Khan, Sara Shujait, Kainat Chaudhary, Muhammad Ikram, Muhammad Imran, Junaid Haider, Maaz Khan, Qasim Khan, and Muhammad Maqbool, *Advances in Colloid and Interface Science*, **300**: 102597 (2022); https://doi.org/10.1016/j.cis.2021.102597
6. Nadeem Baig, Irshad Kammakakam, and Wail Falath, *Materials Advance*, **2**, No. 6: 1821(2021); https://doi.org/10.1039/D0MA00807A
7. Khalaf Ajaj, Mushtaq Abed Al-Jubbori, and Abdullah M. Ali, *Radiation Physics and Chemistry*, **216**: 111384 (2024); https://doi.org/10.1016/j.radphyschem.2023.111384
8. Khalaf Ajaj, Abdullah M. Ali, and Mushtaq Abed Al-Jubbori, *Nanosistemi, Nanomateriali, Nanotehnologii*, **22**, Iss. 1: 209 (2024); https://doi.org/10.15407/nnn.22.01.209
9. Dongshi Zhang, Bilal Gökce, and Stephan Barcikowski, *Chemical Reviews*, **117**, Iss. 5: 3990 (2017); https://doi:10.1021/acs.chemrev.6b00468
10. Dapeng Chen, Xueliang Qiao, Xiaolin Qiu, and Jianguo Chen, *J. Mater. Sci.*, **44**: 1076 (2009); http://doi.org/10.1007/s10853-008-3204-y
11. José S. Garitaonandia, Maite Insausti, Eider Goikolea, Motohiro Suzuki, John D. Cashion, Naomi Kawamura, Hitoshi Ohsawa, Izaskun Gil de Muro, Kiyonori Suzuki, Fernando Plazaola, and Teofilo Rojo, *Nano Lett.*, **8**, Iss. 2:

661 (2008); https://doi.org/10.1021/nl073129g
12. Hao Encai and George C. Schatz, *The Journal of Chemical Physics*, **120**, No. 1: 357 (2004); https://doi.org/10.1063/1.1629280
13. J. J. Mock, M. Barbic, D. R. Smith, D. A. Schultz, and S. Schultz, *J. Chem. Phys.*, **116**, Iss. 15: 6755 (2002); https://doi.org/10.1063/1.1462610
14. Yugang Sun and Younan Xia, *Science*, **298**, Iss. 5601: 2176 (2002); doi:10.1126/science.1077229
15. Adawiya J. Haider, Rusul Abed AL-Rsool, and Mohammad J. Haider, *Plasmonics*, **13**, No. 5: 1649 (2018); https://doi.org/10.1007/s11468-017-0674-2
16. Gang Wei, Hualan Zhou, Zhiguo Liu, and Zhuang Li, *Applied Surface Science*, **240**, Iss. 1–4: 260 (2005); https://doi.org/10.1016/j.apsusc.2004.06.116
17. J. García Solé, L. E. Bausá, and D. Jaque, *An Introduction to the Optical Spectroscopy of Inorganic Solids* (Chichester, England: John Wiley & Sons: 2005); doi:10.1002/0470016043
18. Isha Saini, Jyoti Rozra, Navneet Chandak, Sanjeev Aggarwal, Pawan K. Sharma, and Annu Sharma, *Mater. Chem. Phys*, **139**, Iss. 2–3: 802 (2013); https://doi.org/10.1016/j.matchemphys.2013.02.035
19. M. Rashidian and D. Dorranian, *J. Theor. Appl. Phys.*, **8**: Arcticle No. 121 (2014); https://doi.org/10.1007/s40094-014-0121-0
20. Khalaf Ajaj, Mushtaq Abed Al-Jubbori, and Abdullah M. Ali, *Journal of Laser Applications*, **35**, Iss. 4: 042055 (2023); https://doi.org/10.2351/7.0001221
21. J. Tau, R. Grigorovici, and A. Vancu, *phys. stat. sol. (b)*, **15**, Iss. 2: 627 (1966); https://doi.org/10.1002/pssb.19660150224